Title: Bacteria Inactivation at a Sub-Stoichiometric Titanium Dioxide Reactive Electrochemical Membrane

Author: Lun Guo Kai Ding Karl Rockne Metin Duran Brian P. Chaplin

PII: S0304-3894(16)30489-7
DOI: http://dx.doi.org/doi:10.1016/j.jhazmat.2016.05.051
Reference: HAZMAT 17740

To appear in: *Journal of Hazardous Materials*

Received date: 15-10-2015
Revised date: 27-4-2016
Accepted date: 15-5-2016

Please cite this article as: Lun Guo, Kai Ding, Karl Rockne, Metin Duran, Brian P.Chaplin, Bacteria Inactivation at a Sub-Stoichiometric Titanium Dioxide Reactive Electrochemical Membrane, Journal of Hazardous Materials http://dx.doi.org/10.1016/j.jhazmat.2016.05.051

Bacteria Inactivation at a Sub-Stoichiometric Titanium Dioxide Reactive Electrochemical Membrane

Lun Guo[1], Kai Ding[2], Karl Rockne[3], Metin Duran[2], Brian P. Chaplin[*1]

[1]Department of Chemical Engineering, University of Illinois at Chicago, 810 South Clinton Street, Chicago, Illinois 60607, United States

[2]Department of Civil and Environmental Engineering, Villanova University, 800 Lancaster Ave., Villanova, PA, 19085 United States

[3]Department of Civil and Materials Engineering, University of Illinois at Chicago, 842 W. Taylor St., Chicago, Illinois 60607, United States

* Corresponding author: Phone: 312-996-0288; fax: 312-996-0808; e-mail: chaplin@uic.edu

Highlights

- A reactive electrochemical membrane inactivated *E. coli* in chloride-free solutions.
- Inactivation was attributed to acidic/alkaline boundary layers at the electrodes.
- A low energy requirement (2.0 to 88 W.hr m^{-3}) was found for inactivation.

Abstract

This study investigated the use of a sub-stoichiometric TiO_2 reactive electrochemical membrane (REM) for the inactivation of a model *Escherichia coli* (*E. coli*) pathogen in chloride-free solutions. The filtration system was operated in dead-end, outside-in filtration model, using the REM as anode and a stainless steel mesh as cathode. A 1-log removal of *E. coli* was achieved when the electrochemical cell was operated at the open circuit potential, due to a simple bacteria-sieving mechanism. At applied cell potentials of 1.3 and 3.5 V neither live nor dead *E. coli* cells were detected in the permeate stream (detection limit of 1.0 cell mL^{-1}), which was attributed to enhanced electrostatic bacteria adsorption at the REM anode. Bacteria inactivation in the retentate solution increased as a function of the applied cell potential, which was attributed to transport of *E. coli* to the REM and stainless steel cathode surfaces, and direct contact with the local acidic and alkaline environment produced by water oxidation at the anode and cathode, respectively. Clear evidence for an *E. coli* inactivation mechanism mediated by either direct or indirect oxidation was not found. The low energy requirement of the process (2.0 to 88 W.hr m^{-3}) makes the REM an attractive method for potable water disinfection.

Keywords: Electrochemical disinfection; reactive electrochemical membrane; bacteria

1.0 Introduction

The development of multi-functional reactive electrochemical membranes (REMs) is an active area of research in water treatment. REMs have the potential to extend the traditional roles of membranes beyond separations to include electrochemical reduction and oxidation reactions, as well as enhanced electrostatic rejection of charged species. The majority of the current research in this area is focused on using either mats of carbon nanotubes (CNTs) physically deposited on a membrane surface or blending CNTs with polymeric materials to form composite membranes [1-10]. These techniques have shown exceptional promise towards developing novel multi-functional membranes that have utility in disinfection, organic compound oxidation, and fouling prevention at the bench-scale [1-10]. However, key limitations of CNT-based membrane materials still exist, including: 1) high anodic potentials can lead to corrosion of the CNT network or degradation of the polymeric membrane material [11]; 2) high cost of CNTs (~ \$100 kg^{-1}) [12]; and 3) cytotoxicity of CNTs could potentially pose health risks if they are ingested or released into the environment [13-16].

An alternative electrode material that addresses the key limitations of CNT-based membranes is comprised of the suboxides of TiO_2, collectively known as Magnéli phases (Ti_nO_{2n-1}, $4 \leq n \leq 10$) [17-19]. Stoichiometric titanium dioxide (TiO_2) is an insulator (electrical conductivity ~ 10^{-9} Ω^{-1} cm^{-1}) [20], but the electronic properties of TiO_2 can be changed by creating oxygen deficiencies in the lattice structure through thermal reduction methods, which results in conversion of a fraction of $Ti^{(IV)}$ to $Ti^{(III)}$ and imparts n-type semiconductor behavior [20]. The advantages of Magnéli phase electrodes include: 1) they can be synthesized into porous ceramic materials that are chemically resistant to acids, bases, and oxidants [20]; 2) their low cost, as the precursor TiO_2 material is abundant and cheap (~ \$7 kg^{-1}) [21]; and 3) Ti is broadly

biocompatible and relatively non-toxic, since nanoparticles are not used [22].

Electrochemical inactivation of microorganisms is a viable alternative to traditional disinfection methods [2, 3, 23-27]. Electrochemical inactivation is especially attractive for non-centralized treatment because it is simple, has a low energy requirement, and does not require chemical addition. As a result, research has focused on creating compact, electrochemical technologies for water disinfection [2, 3, 23-25, 28]. There are three primary electrochemically-mediated inactivation mechanisms proposed in the literature: 1) electroporation [28], 2) indirect oxidation [26, 27], and 3) direct oxidation [2, 3, 23-25]. Electroporation is the mechanism by which a strong electric field ($> 10^5$ V cm^{-1}) induces phospholipids in the cell membrane to rearrange, creating pores that can cause cell death [29]. Inactivation by indirect oxidation has been reported to occur via the electrochemical generation of either reactive oxygen species (e.g., $OH^{\bullet}$, H_2O_2, O_3) [26, 27] or electrochemically produced Cl_2 [30], and direct oxidation is the mechanism by which either a protein or functional group in the cell membrane directly injects an electron into the anode. This process creates a radical site in the cell membrane, causing lipid peroxidation, which leads to a series of radical chain reactions that compromise the cell membrane integrity and leads to cell death [31]. Direct oxidation has been proposed in several studies as the primary inactivation mechanism of both bacteria and viruses [2, 3, 23-25]. However, the exact mechanism has never been elucidated.

Expanding on prior work from our group focused on using REMs for organic compound oxidation [19, 32], this study reports on the use of a Ti_nO_{2n-1} ceramic REM for the inactivation of a model pathogen (*Escherichia coli*). A combination of membrane filtration experiments, fluorescent microscopy, and electrochemical methods are used to demonstrate the utility of the

REM for water disinfection and gain information on the possible mechanisms of bacteria inactivation in chloride-free water using this novel electrode material.

2.0 Materials and Methods

2.1 Reagents and Cultures. All chemicals were reagent-grade and obtained from Fisher Scientific (Pittsburgh, PA, USA) and Sigma-Aldrich (St. Louis, MO USA) and used as received. All solutions were made using water from a NANOPure water purification system (Barnstead-Thermolyne, Dubuque, IA USA) with resistivity greater than 18 MΩ·cm (21° C), referred to as DI water. *Escherichia coli* (ATCC 25922) was obtained from the American National Type Culture Collection (Manassas, VA, USA).

2.2 Bacterial Growth Curve. *Escherichia coli* (*E. coli*) was used in this study as a model pathogen. *E. coli* was first resuscitated in 25 g L^{-1} Luria-Bertani (LB) broth (Difco, Detroit, MI) solution for 48 hr at 33 °C. After resuscitation, 1 mL of bacterial suspension was transferred to a test tube with fresh LB broth and 10 mM $NaClO_4$ or 10 mM $NaHCO_3$ electrolyte, and maintained in an incubator at 33 °C, which served as a seed for future inactivation experiments. A typical growth curve experiment consisted of adding 0.1 mL of seed to fresh broth/electrolyte and incubation at 33 °C. Absorbance (A_{600}) of the bacterial suspension was recorded every 20 min with a spectrophotometer (1100RS, UNICO, Dayton, NJ USA), until the growth of bacteria reached the stationary phase (~ 400 min.). A typical growth curve is provided in the Supporting Information (SI) (Figure S-1).

2.3 Plate Count Method. The plate count method used for *E. coli* quantification was a modified version of EPA method 1103.1 [33]. Plates were prepared with LB agar medium according to the manufacturer's instructions and then autoclaved at 121 °C. The agar medium was then poured into 9 × 50 mm culture dishes to a depth of 4-5 mm. Culture fluid was well-

mixed with a vortex shaker (VSM-3 Vortex Mixer, PRO Scientific, Oxford, CT USA), and was diluted to a 10 mL volume with autoclaved DI water using the serial dilution method. A series of dilutions was performed to ensure that between 10 to 300 bacteria colony forming units (CFU) mL^{-1} was obtained in one of the diluted samples. The diluted samples were filtered through a 47 mm diameter, 0.2 μm pore size membrane filter (S-PAK membrane, MILLIPORE, Billerica, MA USA). The membrane was removed from the filter base and rolled onto the agar to avoid bubble formation between the membrane and the agar surface. The plates were cultured in the incubator for ~ 24 hr., after which the individual CFUs were counted.

2.4 Direct Count Method. Direct counts were performed using a fluorescence-based, nucleic acid assay, in which *E. coli* cells were stained with a LIVE/DEAD® *Bac*Light™ bacterial viability kit (Molecular Probes, Inc. Eugene, OR USA) for 15 min in the dark. The kit contains 4',6-diamidino-2-phenylindole (DAPI) and propidium iodide (PI) dyes that were used to determine live (green) and dead (red) cells, respectively. The stained bacteria were imaged with an epifluorescence microscope (Leica Biosystems, DM2000) with a 364 nm filter for imaging cells stained with both PI and DAPI and a 464 nm filter for detecting cells stained with only PI. Ten representative images (0.28 mm x 0.21 mm) from different random locations on each filter were captured for subsequent data analysis through direct counting methods. Area of the microscope field of view was determined using a Ronchi ruling glass slide. At least 200 cells were counted for each experiment, and total cell density was calculated assuming that the ten sample areas were representative of the entire filter area. Results are reported as average ± the 95% confidence interval.

Direct counts were compared to the plate counts by preparing standards containing various proportions of live and dead *E. coli* cells. Live and dead *E. coli* standards were prepared by

growing the bacteria to late-log phase. Aliquots of the bacterial suspension were placed into "*live"* and "*dead"* test tubes. Ethanol was added to the *dead* cell tube and was allowed to mix for 15 min. The *dead* cell tube was centrifuged and washed with DI water three times and the cell pellet was re-suspended in DI water. Standards were prepared by mixing liquid aliquots from the *live* cell tube and *dead* cell tube in order to obtain proportions of live:dead cells of 100:0, 75:25, 50:50, 25:75, and 0:100. Bacteria numbers for these standards were determined by both direct count and plate count methods. A two-tail t-test was performed on the sample means obtained from the two methods and results indicate that they were not statistically different (Supporting Information; Figures S-2-S-5).

2.5 Reactive Electrochemical Membrane (REM). The REM was a sub-stoichiometric TiO_2 electrode that was used as received from Vector Corrosion Technologies Inc. (Wesley Chapel, FL USA). The REM had a 10 mm outer membrane, 7.5 mm inner diameter, and 10 cm length. The median pore diameter was 1.7 μm and porosity was ~30% [19]. The REM was characterized by scanning electrochemical microscopy (SEM) using a Hitachi S-4800 cold field emission SEM (Hitachi High Technologies America, Inc., Schaumburg, IL USA), and X-ray diffraction (XRD) using a Siemens D-5000 (Siemens/Bruker, Billerica, MA USA) instrument with a Cu X-ray tube (40 kV and 25 mA).

2.6 Membrane Filtration Experiments. The sub-stoichiometric TiO_2 electrode was used as the REM anode (30 cm^2) and was arranged in the center of the feed tank (Figure 1). A stainless steel mesh (132 cm^2) surrounding the REM was used as the cathode (~ 1.0 cm electrode spacing). An aliquot of the bacterial suspension, grown to late-log phase (A_{600} = 0.8-1.0), was added to a 10 mM $NaClO_4$ solution to prepare the feed solution for the filtration test. An initial *E coli* concentration of ~ 10^4 CFU mL^{-1} was used for all filtration experiments. Membrane

filtration was operated in the outside-in, dead-end flow mode. The reactor was filled with 0.8 L of electrolyte containing the bacterial suspension (feed solution), and a peristaltic pump was used to draw the solution from the reactor, through the REM, and to the permeate tank. The feed solution was added to the reactor at the same rate as permeate was withdrawn. A pumping rate of ~ 10 mL min^{-1} was used, which correlated to a normalized membrane flux of 200 L m^{-2} hr^{-1} (LMH). The reactor was stirred continuously with a magnetic stir bar for the duration of the experiment. Permeate samples were collected in autoclaved glass beakers. Cell potentials of 0, 1.3, and 3.5 V were applied using a direct power supply (Protek Test and Measurement, P6035, Incheon, Korea), and the potentials of the anode and cathode were monitored versus the Ag/AgCl reference electrode. All potentials are reported versus the standard hydrogen electrode (SHE) and corrected for the ohmic drop due to solution resistance. The 1.3 V cell potential corresponded to an anode potential of 1.0 V/SHE, a cathodic potential of -0.3 V/SHE, a negligible ohmic drop, and a current of approximately 1.0 mA (anodic current density = 0.03 mA cm^{-2}; cathodic current density = 0.007 mA cm^{-2}). The 3.5 V cell potential corresponded to an anode potential of 2.0 V/SHE, a cathodic potential of -1.0 V/SHE, ohmic drop of 0.5 V, and a current of approximately 15 mA (anodic current density = 0.50 mA cm^{-2}; cathodic current density = 0.11 mA cm^{-2}). The open circuit potential (OCP) of the anode was ~ 0.4 V/SHE.

The surface area normalized power consumption (P) and liquid volume normalized energy requirement ($\bar{E}$) of the REM during filtration experiments was calculated according to equations (1) and (2), respectively.

$$P = V_{cell} * j \quad (1)$$

$$\bar{E} = P/J \quad (2)$$

where V_{cell} is the cell potential; j is the current density that is normalized by the geometric surface area of the REM; and J is the permeate flux normalized by the geometric surface area of the REM.

Bacteria concentrations were determined by both plate count and direct count methods in four samples: 1) initial feed solution, 2) permeate solution, 3) reactor solution at end of the experiment ("retentate"), and 4) backflush solution. The backflush solution was obtained after each experiment and consisted of back flushing the REM with 100 mL of sterile DI water. After each experiment the REM and tubing were cleaned by back flushing with 100 mL of isopropyl alcohol and 1 L of DI water in succession, and the glass reactor was autoclaved. All filtration experiments were performed in triplicate and results are reported as averages with error bars representing the high and low values.

2.7 Batch Inactivation Experiments. Batch experiments were performed using a divided cell reactor with a Nafion membrane (Ion Power, Inc., New Castle, DE) separating the two liquid chambers (see SI, Figure S-6). Both chambers were filled with an initial *E. coli* concentration of ~ 10^5 CFU mL^{-1}. The larger chamber was filled with 125 mL bacterial suspension and used to test the working electrode; the smaller chamber was filled with 50 mL bacterial suspension and used for placement of the counter electrode. In order to increase ionic strength, 10 mM of $NaClO_4$ or $NaHCO_3$ was also added to solution. A direct power supply was used to apply the cell potential, and the anodic or cathodic potentials of the working electrode were monitored using a Ag/AgCl reference electrode and were corrected for solution resistance and reported versus the SHE. In order to mimic electrode potentials observed in filtration experiments, batch experiments were conducted using the REM as working electrode at anodic potentials of 1 and 2 V/SHE and the stainless steel mesh as working electrode at cathodic

potentials of -0.3 and -1 V/SHE. Each experiment lasted for 2 hours and samples were taken at 15 min intervals and bacteria were quantified by the plate count method. All experiments were performed in triplicate at room temperature (21-22 ^{o}C) using late-log phase bacteria, and results are reported as averages with error bars representing the high and low values. Control experiments without an applied potential were performed in parallel.

2.8 Control Experiments. The effect of solution pH on bacteria inactivation was assessed by conducting batch experiments in a beaker containing 100 mL of 10 mM $NaClO_4$ electrolyte solution with an initial *E. coli* concentration of ~ 10^5 CFU mL^{-1}. The pH was varied from the initial pH (~6.0) to pH ~ 2 by the drop-wise addition of 0.1 M $HClO_4$, and from the initial pH to pH ~ 12 by the drop-wise addition of 0.1 M NaOH. The bacteria suspension was stirred for 10 minutes at each pH value prior to bacteria quantification using the plate count method. Control experiments were performed in parallel at pH = 6.

A blank sample was analyzed for *E. coli* before each bacteria inactivation experiment. A blank sample was obtained as follows. Autoclaved DI water was placed in the autoclaved reactor with the cleaned electrodes for approximately 10 min and then plate counts of subsamples were taken. Bacteria were never observed in any of these blank samples, indicating that the cleaning protocol was sufficient.

2.9 Electrochemical Measurements. Linear sweep voltammetry (LSV) was used to characterize a mass transport rate constant (k_m) to the REM surface using the limiting current (i_{lim}) method described by equation (3) [19].

$$k_m = \frac{i_{lim}}{nFAC} \quad (3)$$

where $n = 1$ is the number of electrons transferred; F is the Faraday constant; A is the geometric surface area of the electrode; and C is the concentration of the $K_4Fe(CN)_6$ redox species (5 mM).

Cyclic voltammetry (CV) scans were conducted to measure the nonfaradaic current and ascertain the double layer capacitance (C_d) of the REM in a 1 M $NaClO_4$ electrolyte. Electrochemical impedance spectroscopy (EIS) was used to determine the solution resistance between the working electrode and the Ag/AgCl reference electrode and allowed for correction of the measured potentials for solution resistance. All electrochemical measurements were made using a Gamry Reference 600 Potentiostat (Gamry Instruments, Warminster, PA USA). EIS measurements were performed at the OCP, with a 10 mV alternating voltage signal, and over a frequency range of 0.1 Hz to 10 kHz. The electrochemical data were analyzed by Gamry Echem Analyst software (v6.01, Warminster, PA).

2.10 Analytical Methods. Solution phase oxidants were monitored using a hydrogen peroxide test kit (Model HYP-1, HACH). The kit utilized the sodium thiosulfate titration method, which detects any species that can oxidize thiosulfate ($E^o = 0.08$ V). Therefore, the method is used as an indicator of total solution phase oxidants, with a detection limit of 5.7 μM. Terephthalic acid oxidation to form 2-hydroxyterephthalic acid was used as the $OH^{\bullet}$ probe reaction [34]. Concentrations of terephthalic acid were determined using HPLC with a C18 (2) column (250 x 4.6 mm, Luna) and a photodiode array detector (wavelength = 254 nm) (SPD-M30A, Shimadzu Corp., Kyoto, Japan). HPLC with a fluorescent detector (RF-20A, Shimadzu) was used for quantification of 2-hydroxyterephthalic acid (λ_{ex} = 315 nm and λ_{em} = 435 nm). The pH and temperature were measured using a multi-function meter and probe (PC2700, Oakton Instruments, Vernon Hills, IL USA).

3.0 Results and Discussion

3.1 REM Characterization. The surface morphology of the REM was characterized by SEM, and results indicate surficial pores on the order of 1—5 μm (Figure 2a). XRD data in Figure 2b shows peaks characteristic of TiO_2 and Ti_9O_{17}, indicating the presence of the Magnéli phase [20]. The phases detected by XRD are consistent with the measured electrical conductivity of the REM [20], which was approximately 50 S m^{-1}. The k_m to the REM surface was characterized in the presence and absence of a membrane flux using equation 3, and results are shown in Figure 2c. The peak current due to the oxidation of $Fe(CN)_6^{4-}$ at approximately 1.6 V was over an order of magnitude greater at a membrane flux of 243 LMH relative to well-stirred batch conditions, corresponding to an increase in the k_m value from 10 to 256 LMH (2.9×10^{-6} to 7.1×10^{-5} m s^{-1}), respectively. The value for k_m determined under pumping conditions is similar to other electrochemical flow-through reactors that reported k_m values between 10^{-5} and 10^{-4} m s^{-1} [19, 32, 35, 36]. The similarity between the measured value for membrane flux (243 LMH) and the measured k_m during pumping (256 LMH) indicates that convection limits mass transport to the REM surface. This result is consistent with our prior work that showed a 1:1 relationship between k_m and the measured membrane flux over a range of flux values (30-102 LMH) [19]. The high measured k_m value is not due to the high surface area of the REM. If this were the case, the k_m value would exceed the value measured for membrane flux.

However, a high REM surface area could enhance the adsorption capacity for bacteria. Therefore, CV scans were conducted in a 1 M $NaClO_4$ electrolyte to measure the nonfaradaic current and ascertain the C_d of the REM (Figure 2d), which is a measure of the electroactive surface area. At a scan rate (υ) of 0.1 V s^{-1} it was determined that the 30 cm^2 REM had a C_d value of 0.2 F. The electroactive surface area was determined as 3333 cm^2, which was obtained

by dividing C_d by 60 μF cm^{-2}; consistent with the well accepted value for the double layer capacitance of metal oxides [37]. The estimated roughness factor (ratio of electroactive surface area to nominal geometric surface area) was 111, which is comparable to prior studies with porous electrodes [19, 38], indicating that the REM possesses an enhanced reactive surface area that can be utilized by the novel flow-through operation for bacteria adsorption and inactivation.

3.2 Bacteria Filtration Experiments. Filtration experiments were conducted to evaluate both the separation and inactivation of *E. coli* by the REM as a function of cell potential. The initial feed concentration of bacteria for filtration experiments was ~ 10^4 CFU mL^{-1}, and experiments were conducted at cell potentials of 0, 1.3, and 3.5 V, which corresponded to anodic potentials of 0.4, 1.0 and 2.0 V/SHE, respectively. Figure 3a shows results for *E. coli* plate counts for the initial, retentate, permeate, and backflush solutions. Representative *E. coli* images taken by fluorescent microscopy of these four solutions after staining with BacLight® live/dead dyes are shown in Figures 3b-d. Comparison of plate and direct counts were consistent, as there was not a significant difference in the number of live cells quantified by the two methods (SI, Figures S-7, S-8, and S-9). A total cell balance was performed using the direct count method, and results indicate that cell numbers were conserved before and after the experiments (SI, Figure S-10).

A 1-log removal of bacteria was observed in the permeate solution in the absence of an applied potential (Figure 3a), which was attributed to bacteria adsorption and size exclusion separation. The average pore size of the REM is 1.7 μm and similar in size to *E coli.* cells, which are rod shaped and on the order of 2.0 μm x 0.5 μm [39]. However, the high tortuosity of the REM enhances its filtration capacity beyond simple straining, and replicate experiments without an applied potential consistently obtained a 1-log separation of *E. coli* cells. By contrast, bacteria

were neither detected by the plate count method (detection limit = 1.0 CFU mL^{-1}) nor by fluorescent microscopy (detection limit = 30 cells mL^{-1}) in the permeate solutions when applying cell potentials of either 1.3 or 3.5 V. The absence of both live and dead cells in the permeate solution indicates that the application of an electrode potential enhances the filtration capacity of the REM. The enhanced separation of *E. coli* in the permeate during filtration experiments in the presence of an applied potential indicates electrostatics may have affected cell transport through the REM. Electrostatic interactions between the positively charged REM surface induced by an anodic potential and the negatively charged *E. coli* cells would result in increased adsorption of cells at the REM surface, thus preventing transport through the REM. The isoelectric point of *E. coli* has been reported at ~ 2.0 [40], and therefore *E. coli* cells would be negatively charged at both the pH of the bulk solution (pH ~ 5.5-7.5) and the pH at the REM surface during the filtration experiments. The pH at the REM surface was assumed to be similar to the pH observed in the permeate solution, which was ~ 5.2 at the 1.3 V cell potential experiments and dropped to ~ 3.50 at the 3.5 V cell potential experiments (representative pH profiles are shown in Figure S-11).

Only live *E. coli* cells were detected in the retentate solutions in the absence of a cell potential (Figure 3b). However, the number of dead *E. coli* cells in the retentate increased greatly with an applied cell potential. At a cell potential of 1.3 V there were an average of 7.6×10^5 live cells (25 ± 19%) and 2.3×10^6 dead cells (75 ± 25 %) determined by fluorescent microscopy. In contrast, live cells were not detected and an average of 3.5×10^6 dead cells were detected by fluorescent microscopy at a cell potential of 3.5 V. During backflush of the REM the distribution between live and dead cells was approximately equal. At 1.3 V cell potential (1.0 V/SHE anodic potential) there were an average of 5.9×10^4 live cells (44 ± 10%) and 7.5×10^4 dead cells (56 ±

12%). At 3.5 V cell potential (2.0 V/SHE anodic potential) there were an average of 5.1 x 10^4 live cells (65 ± 14%) and 2.8 x 10^4 dead cells (35 ± 8%). These results indicate that *E. coli* adsorption to the REM did not always lead to cell death, and suggest that either bulk solution phase species may be responsible for cell death or the bacteria deposit in multi-layers on the REM and only a portion of these cells was killed by processes occurring at the electrode surface.

Solution phase chemical conditions that could lead to *E. coli* death include formation of extremely acidic or basic pH or the production of reactive oxygen species (ROS) [41]. The pH of the retentate solution was approximately 5.5-7.5 and did not change drastically during any of the filtration experiments. Production of solution phase oxidants was monitored by thiosulfate titration and results were always below the method detection limit (5.7 μM). The lack of a positive detection indicates that the reactor did not contain significant bulk concentrations of any thiosulfate reactive solution phase oxidants. However, the high cell deaths observed in the retentate, compared to only partial cell deaths in the backwash suggest that local solutions conditions near the cathode surface may be contributing to *E. coli* inactivation. The production of H_2O_2 and OH^- at the cathode surface, according to reactions (4) and (5), respectively, could contribute to cell inactivation. The mixing in the reactor would allow significant contact time between the *E. coli* cells and the high surface area cathode surface, and prior work indicates that significant pH and H_2O_2 gradients can exist at electrode surfaces [42, 43].

$$O_2 + 2H^+ + 2e^- \rightarrow H_2O_2 \quad (4)$$

$$2H_2O + 2e^- \rightarrow H_2 + 2OH^- \quad (5)$$

3.3 Batch Experiments. In the bacteria filtration experiments (Figure 3), the anode and cathode were in the same reactor chamber. Therefore, in order to obtain information regarding

the individual functions of the anode and cathode during disinfection, batch experiments were conducted in a divided cell reactor (see SI, Figure S-6). Divided cell batch experiments were conducted to assess oxidant formation and the individual roles that the anode and cathode may have on *E. coli* inactivation. The close agreement between plate counts and direct counts (SI, Figures S-7, S-8, S-9) is consistent with an inactivation mechanism involving the deterioration of the cell membrane. Electroporation is unlikely to be responsible for the observed cell inactivation in our study, due to the low electric field strengths used in our experiments (i.e., 1.3-3.5 V cm^{-1}). Thus it is likely that either an oxidation-mediated mechanism or some as yet unknown process was responsible for the observed results. Additional electrochemical experiments were performed to explore the role of both direct and indirect oxidation mechanisms on bacteria inactivation.

Indirect oxidation of bacteria cells can be initiated by the electrochemical production of oxidants at the anode or cathode surface. Since the $NaClO_4$ electrolyte is electrochemically inert [44, 45], indirect oxidation could be facilitated by the generation of ROS. In addition to H_2O_2 formation at the cathode, ROS formation can be initiated at the anode (i.e., $OH^{\bullet}$, H_2O_2, and O_3) according to the following reactions [46-50]:

$$H_2O \rightarrow OH^{\bullet} + H^+ + e^- \quad (6)$$

$$2OH^{\bullet} \rightarrow H_2O_2 \quad (7)$$

$$2OH^{\bullet} \rightarrow O_{2(ads)} + 2H^+ + 2e^- \quad (8)$$

$$OH^{\bullet} + O_{2(ads)} \rightarrow HO^{\bullet}_{3(ads)} \quad (9)$$

$$HO^{\bullet}_{3(ads)} \rightarrow O_3 + H^+ + e^- \quad (10)$$

Since these oxidants are formed at the electrode/electrolyte interface, their concentrations will be greatest adjacent to the electrode surface and depending on their reactivity may not increase to detectable levels in the bulk solution. It is well documented that radical species (e.g., $OH^{\bullet}$) only exist at appreciable concentrations a few microns from the electrode surface [50, 51]. Less reactive oxidants like O_3 and H_2O_2 are often detected in the bulk solution, but studies have also shown that significant concentration gradients exist at the electrode surface [43].

Divided cell experiments, which separated the anode and cathode with a Nafion membrane, were conducted to assess ROS production at the REM anode and stainless steel cathode in a 100 mM $NaClO_4$ electrolyte and in the absence of bacteria. The production of $OH^{\bullet}$ □□s assessed using terephthalic acid as an $OH^{\bullet}$ p□□□□, and the production of total oxidants was assessed using the thiosulfate titration method. Terephthalic acid oxidation was not observed at anodic potentials of either 1.0 or 2.0 V/SHE, and total oxidant production was below the detection limit (5.7 μM) of the thiosulfate method (data not shown). These results indicate that significant concentrations of ROS species were not produced via water oxidation at the anode, which is not surprising since ROS formation is dependent on $OH^{\bullet}$ formation (E^{o} = 2.59 V/SHE), whose redox potential is well above the anodic potentials used in this study [52]. Cathodic divided cell experiments with the stainless steel mesh at -1.0 V/SHE resulted in the detection of a total oxidant concentration of 8.5 and 10 μM at the conclusion of the 2-hour duplicate experiments, indicating that low levels of oxidants were formed on the cathode, although it is not clear if these levels were sufficient to contribute to *E. coli* inactivation. The lack of detection of oxidants during bacteria filtration experiments could be related to reaction of H_2O_2 with bacteria cells. Studies have shown that a steady state concentration of H_2O_2 of ~ 25 μM existed approximately 50 μm from a cathode surface, and this concentration was capable of preventing biofilm growth

on the electrode [43]. However, concentrations of H_2O_2 were not detected at distances > 400 μm from the cathode surface [43].

In order to determine if direct oxidation was a possible mechanism for *E. coli* inactivation, experiments were conducted using a 10 mM $NaHCO_3$ electrolyte (pH = 8.0), where HCO_3^- and CO_3^{2-} ions are used to quench low concentrations of $OH^{\bullet}$ that may form on the anode surface [53]. Anodic potentials of both 1.0 and 2.0 V/SHE were tested. The pH of the solution (pH ~ 8.0) was relatively stable during the duration of the 1 V/SHE experiments, and decreased to approximately 7.0 for anodic experiments at 2.0 V/SHE. In all of these experiments, discernable *E. coli* inactivation was not observed (data not shown). These results suggest that direct oxidation was not a significant mechanism for *E. coli* inactivation in divided cell experiments, and thus is also an unlikely mechanism during the filtration experiments.

Additional divided cell experiments were conducted to determine if *E. coli* inactivation occurred at either the anode or cathode under potentials representative of the filtration experiments. For these experiments anode potentials of 1.0 and 2.0 V/SHE and cathode potentials of -0.3 and -1.0 V/SHE were tested. Figure 4 shows data for triplicate batch experiments using the REM as the working electrode at an anodic potential of 1.0 V/SHE (Figure 4a) and at 2.0 V/SHE (Figure 4b) in a 10 mM $NaClO_4$ electrolyte. *E. coli* concentrations were similar to the control in the 1.0 V/SHE experiments, but *E. coli* concentrations steadily declined with increased reaction time in the 2.0 V/SHE experiments. The pH in the anode chamber decreased during the experiments due to the presence of the Nafion membrane separator. During the 1.0 V/SHE anodic experiments the pH decreased from an initial value of ~ 6.0 to a pH of ~ 4.8±0.2 at the conclusion of the triplicate experiments (Figure 4a and 4b). During the 2.0 V/SHE

anodic experiments the pH decreased from an initial value of ~ 6.2 to a final pH of 2.3±0.2, suggesting that the acidic pH may be the cause for *E. coli* inactivation [54, 55].

Divided cell experiments were also conducted using the stainless steel mesh as the working electrode at cathodic potentials of -0.3 and -1.0 V in the 10 mM $NaClO_4$ electrolyte (Figure 5). The inactivation of *E. coli* cells was not observed in the -0.3 V/SHE experiments (Figure 5a), but was observed during the -1.0 V/SHE experiments (Figure 5b). Once again the pH was observed to increase from the initial value of ~ 6.0 to 7.9±0.2 at the conclusion of the -0.3 V/SHE triplicate experiments. For the -1.0 V/SHE experiments the pH increase was more dramatic, reaching a final pH of 11.3±0.1 in the triplicate experiments. Cathodic experiments were repeated using 10 mM $NaHCO_3$ electrolyte to buffer the pH. As with anodic experiments using the $NaHCO_3$ electrolyte, bacteria inactivation was not observed. The pH was relatively stable at pH = 8.0 during the -0.3 V/SHE experiments and increased to pH = 9.5±0.2 at the conclusion of the -1.0 V/SHE experiments.

Batch experiments were also conducted containing only bacteria and the 10 mM $NaClO_4$ electrolyte, and without the electrochemical cell to further validate the role of pH in bacteria inactivation. The solution was titrated with either 0.1 M $HClO_4$ or 0.1 M NaOH and *E. coli* concentrations were quantified at various pH values. Results indicate that the viable bacteria numbers decreased when the pH decreased below 2.89 or increased above 9.55 (Figure 6), and nearly all the bacteria were inactivated at the final pH values of 2 and 12. These results further support the hypothesis that pH change was the primary mode of bacteria inactivation during batch inactivation experiments, which is consistent with the literature [27, 41, 56]. Bacteria cells must maintain a neutral intracellular pH to prevent: 1) destruction of acid and alkaline labile macromolecules—for example DNA is acid labile and RNA is alkaline labile, and 2)

denaturing of proteins. The change in solution pH causes a rapid change in the internal pH of the cell. In order to maintain a neutral intracellular pH, the bacteria attempts to either pump protons in or out of the cell. Under extreme pH conditions the bacteria may not generate the necessary ATP to maintain a neutral intracellular pH. A prolonged acidic or alkaline intracellular pH ultimately will result in cell death, caused by a destruction of intracellular macromolecules. In addition, extreme extracellular pH may interfere with the proton motive force that bacteria rely on for ATP synthesis [56].

3.4 Inactivation Mechanisms. Based on the experimental evidence it is clear that the generation of H^+ on the anode and OH^- on the cathode were responsible for *E. coli* inactivation during divided cell batch experiments. Translating these results to filtration experiments is complicated by the fact that the pH in the retentate of the filtration reactor was approximately neutral (pH ~ 5.5-7.5) and within the range of *E. coli* viability ($3 < pH < 9$, Figure 6). A possible explanation for these results is related to the different hydrodynamic conditions in the two reactors and the pH and oxidant gradients that can form at the electrode surfaces. The batch reactor was well mixed and utilized a Nafion membrane separator that isolated the anode from the cathode. In this configuration the bulk solution pH increased in the cathode compartment and decreased in the anode compartment with time and resulted in cell death that was easily correlated with the bulk solution pH. However, in the filtration experiments the reactor was operated as a completely stirred tank reactor and without a membrane separator. Therefore, the bulk pH was relatively stable, but significant pH gradients at the electrode surfaces exist.

To explore the possible pH gradients, the surface pH (pH_s) of the cathode was estimated by the following equation [42]:

$$pH_s = 14 - \log\left(OH_b^- + \frac{\gamma j}{nFk_m 1000}\right) \quad (11)$$

where OH_b^- is the bulk OH^- concentration (~10^{-7} M), j is the current density, γ is the fraction of current directed towards the water oxidation reaction (γ = 1), and n is the number of electrons transferred per mole of OH^- generated (n =1, from equation 5). Using the k_m value determined in the filtration reactor for the cathode (k_m = 2.1 x 10^{-6} m s^{-1}), yielded a pH_s = 10.5 at a -0.3 V/SHE cathode potential (j = 0.07 A m^{-2}) and pH_s = 11.7 at a -1.0 V/SHE cathode potential (j = 1.1 A m^{-2}). Therefore, cells coming into contact with the cathode would experience these high pH conditions, which were shown to be sufficiently alkaline to cause cell deaths in control experiments (Figure 6). There is also the possibility of sufficient local H_2O_2 concentrations at the cathode surface that may have contributed to cell inactivation, as was reported previously [43]. However, in our system local H_2O_2 concentrations were not quantified at the cathode surface, so this hypothesis was not tested.

A similar analysis on the anode is complicated by the fact that the acidic boundary layer at the anode is pumped through the REM, as was confirmed by the pH profiles in the permeate (see Figure S-11). An analytical solution was developed that accounted for the convection, diffusion, and H^+ production at the anode surface, which is given below (equation 12) and is discussed in detail in the Supporting Information.

$$C(\bar{x}) = \frac{j\delta}{FD_H Pe}[\exp(Pe) - \exp(Pe\,\bar{x})] + C_b \quad (12)$$

In equation 12, $C(\bar{x})$ is the concentration of H^+ in the boundary layer; $\bar{x}$ is the dimensionless distance in the boundary layer; D_H is the diffusion coefficient for H^+ (9.35 x 10^{-9} m^2 s^{-1}); Pe is the Peclet number $\left(\frac{v\delta}{D_H}\right)$; δ is the thickness of the boundary layer (256 μm); v is the velocity in

the boundary layer due to REM filtration; and C_b is the bulk H^+ concentration (10^{-4} mol m^{-3}). The pH profiles in the boundary layer at the respective current densities observed during filtration experiments with anodic potentials of 1.0 and 2.0 V/SHE are shown in Figure 7. Results indicate pH_s values of 4.4 and 3.2 at anodic potentials of 1.0 and 2.0 V/SHE, respectively. The pH gradient increases at the edge of the boundary layer, which indicates H^+ flux into the bulk solution. This result is supported by the observation that the bulk pH increased only marginally during filtration experiments. Thus, the OH^- generated on the cathode surface was approximately balanced by the flux of H^+ from the anode and into the bulk solution. Since the fluid dynamics in the reactor were not fully characterized, a more quantitative comparison with experimental results was not possible. However, the experimental pH values in the permeate of filtration experiments (Figure S-11) were close to the pH_s values determined by equation 12. At a 1.0 V/SHE anodic potential the permeate pH was 5.2 compared to the calculated value of $pH_s = 4.4$, and at a 2.0 V/SHE anodic potential the permeate pH was 3.5 compared to the calculated value of $pH_s = 3.2$.

The experimental cell viability vs. pH data shown in Figure 6 indicate that *E. coli* cells were inactivated at pH values < 3.0. During filtration experiments the cells had prolonged contact time with the REM (120 minutes), which could have resulted in a higher proportion of cell inactivation then observed in control experiments at a similar pH (contact time = 10 min). Therefore, it is possible that the local acidic conditions that developed at the REM during filtration experiments at an anodic potential of 2.0 V/SHE contributed to cell inactivation. Additionally, the operation of the REM in filtration mode promoted *E. coli* transport to and adsorption on the REM anode. The measured k_m for the REM during filtration experiments in filtration mode ($k_m = 7.1 \times 10^{-5}$ m s^{-1}) was over an order of magnitude higher than that in batch

mode (k_m = 2.9 x 10^{-6} m s^{-1}). The convection-enhanced transport of *E. coli* to the REM surface would place the cells directly at the source of H^+ from water electrolysis and they would also be exposed to low levels of oxidants that may be generated at the anode surface by reactions 6-10. The complexity of the system will likely result in multiple mechanisms for inactivation, and thus more research is needed to fully characterize the mechanisms responsible for bacteria inactivation at electrode surfaces.

3.5 Energy Requirements. The power requirement (equation 1) to operate the REM electrochemical filtration cell was very small; estimated at 0.39 and 17.5 W m^{-2} membrane for the 1.3 and 3.5 V cell potentials, respectively. With an average membrane flux of 200 LMH, this translates to an energy requirement (equation 2) of 2.0 and 88 Wh m^{-3} of solution filtered for the 1.3 and 3.5 V cell potentials, respectively. These energy requirements are negligible when compared to pumping requirements. Several studies have documented the ability of electrochemical reactors to achieve multi-log removal of various bacteria strains, in both the presence and absence of chloride in the source water [57-63]. However, few studies reported on the energy requirements per unit volume of water treated. The lowest reported energy requirement, to our knowledge, was ~ 0.3 kWh m^{-3} for > 6.0 $\log_{10}$ removal of E. coli. in an electrochemical flow-through reactor that produced free chlorine from chloride [57]. Our estimate is 3.4 to 150-fold lower than that reported previously for an electrochemical method, and is comparable to the energy requirement for UV water disinfection at a full-scale drinking water plant (16 Wh m^{-3}) [64].

4.0 Conclusions.

Results from this study indicate that a sub-stoichiometric TiO_2 REM was effective for inactivation of a model *E. coli* pathogen in chloride-free solutions. The REM was operated in dead-end, outside-in filtration model, and bacteria removal was assessed as a function of cell potential. A 1-log removal of *E. coli* was achieved at the open circuit potential, which was attributed to the sieving of bacteria in the REM pores. Neither live nor dead *E. coli* cells were detected in the permeate at cell potentials of 1.3 and 3.5 V. Cell separation was attributed to bacteria adsorption at the positively charged REM anode. Bacteria inactivation in the retentate solution increased as a function of cell potential. Batch experiments provided clear evidence that bacteria inactivation was caused by the production of acidic and basic conditions via water electrolysis reactions at the anode and cathode, respectively. Compelling evidence for an *E. coli* inactivation mechanism mediated by either direct or indirect oxidation was not found. The REM achieved a very low energy requirement for inactivation (2.0 to 88 Wh m^{-3}), which makes it attractive for potable water disinfection.

Acknowledgements. This work was supported by the National Science Foundation (CBET-1356031) and CBET-1453081 (CAREER)). We thank Mr. Joe Tijerina for assistance with experimental work.

References.

[1] A.S. Brady-Estevez, M.H. Schnoor, C.D. Vecitis, N.B. Saleh, M. Ehmelech, Multiwalled Carbon Nanotube Filter: Improving Viral Removal at Low Pressure, Langmuir, 26 (2010) 14975-14982.
[2] C.D. Vecitis, M.H. Schnoor, M.S. Rahaman, J.D. Schiffman, M. Elimelech, Electrochemical Multiwalled Carbon Nanotube Filter for Viral and Bacterial Removal and Inactivation, Environmental Science & Technology, 45 (2011) 3672-3679.
[3] M.S. Rahaman, C.D. Vecitis, M. Elimelech, Electrochemical Carbon-Nanotube Filter Performance toward Virus Removal and Inactivation in the Presence of Natural Organic Matter, Environmental Science & Technology, 46 (2012) 1556-1564.
[4] C.-F. de Lannoy, D. Jassby, K. Gloe, A.D. Gordon, M.R. Wiesner, Aquatic Biofouling Prevention by Electrically Charged Nanocomposite Polymer Thin Film Membranes, Environmental Science & Technology, 47 (2013) 2760-2768.
[5] C.F. de Lannoy, D. Jassby, D.D. Davis, M.R. Wiesner, A highly electrically conductive polymer-multiwalled carbon nanotube nanocomposite membrane, Journal of Membrane Science, 415 (2012) 718-724.
[6] W. Duan, A. Dudchenko, E. Mende, C. Flyer, X. Zhu, D. Jassby, Electrochemical mineral scale prevention and removal on electrically conducting carbon nanotube - polyamide reverse osmosis membranes, Environmental Science-Processes & Impacts, 16 (2014) 1300-1308.
[7] A.V. Dudchenko, J. Rolf, K. Russell, W. Duan, D. Jassby, Organic fouling inhibition on electrically conducting carbon nanotube-polyvinyl alcohol composite ultrafiltration membranes, Journal of Membrane Science, 468 (2014) 1-10.
[8] Q. Zhang, C.D. Vecitis, Conductive CNT-PVDF membrane for capacitive organic fouling reduction, Journal of Membrane Science, 459 (2014) 143-156.
[9] G. Gao, Q. Zhang, C.D. Vecitis, CNT-PVDF composite flow-through electrode for single-pass sequential reduction-oxidation, Journal of Materials Chemistry A, 2 (2014) 6185-6190.
[10] A. Zhu, H.K. Liu, F. Long, E. Su, A.M. Klibanov, Inactivation of Bacteria by Electric Current in the Presence of Carbon Nanotubes Embedded Within a Polymeric Membrane, Applied Biochemistry and Biotechnology, 175 (2015) 666-676.
[11] H. Liu, A. Vajpayee, C.D. Vecitis, Bismuth-Doped Tin Oxide-Coated Carbon Nanotube Network: Improved Anode Stability and Efficiency for Flow-Through Organic Electrooxidation, Acs Applied Materials & Interfaces, 5 (2013) 10054-10066.
[12] M.F.L. De Volder, S.H. Tawfick, R.H. Baughman, A.J. Hart, Carbon Nanotubes: Present and Future Commercial Applications, Science, 339 (2013) 535-539.
[13] S. Kang, M.S. Mauter, M. Elimelech, Physicochemical determinants of multiwalled carbon nanotube bacterial cytotoxicity, Environmental Science & Technology, 42 (2008) 7528-7534.
[14] S. Kang, M.S. Mauter, M. Elimelech, Microbial Cytotoxicity of Carbon-Based Nanomaterials: Implications for River Water and Wastewater Effluent, Environmental Science & Technology, 43 (2009) 2648-2653.
[15] A.L. Alpatova, W.Q. Shan, P. Babica, B.L. Upham, A.R. Rogensues, S.J. Masten, E. Drown, A.K. Mohanty, E.C. Alocilja, V.V. Tarabara, Single-walled carbon nanotubes dispersed in aqueous media via non-covalent functionalization: Effect of dispersant on the stability, cytotoxicity, and epigenetic toxicity of nanotube suspensions, Water Research, 44 (2010) 505-520.
[16] M.S.P. Boyles, L. Young, D.M. Brown, L. MacCalman, H. Cowie, A. Moisala, F. Smail, P.J.W. Smith, L. Proudfoot, A.H. Windle, V. Stone, Multi-walled carbon nanotube induced frustrated phagocytosis, cytotoxicity and pro-inflammatory conditions in macrophages are length dependent and greater than that of asbestos, Toxicology in Vitro, 29 (2015) 1513-1528.

[17] D. Bejan, J.D. Malcolm, L. Morrison, N.J. Bunce, Mechanistic investigation of the conductive ceramic Ebonex (R) as an anode material, Electrochim. Acta, 54 (2009) 5548-5556.
[18] D. Bejan, E. Guinea, N.J. Bunce, On the nature of the hydroxyl radicals produced at boron-doped diamond and Ebonex (R) anodes, Electrochim. Acta, 69 (2012) 275-281.
[19] A.M. Zaky, B.P. Chaplin, Porous Substoichiometric TiO2 Anodes as Reactive Electrochemical Membranes for Water Treatment, Environmental Science & Technology, 47 (2013) 6554-6563.
[20] P.C.S. Hayfield, Development of a New Material - Monolithic Ti4O7 Ebonex® Ceramic, in, Royal Society of Chemistry: Cambridge, UK, 2002.
[21] J. Nowotny, Oxide Semiconductors for Solar Energy Conversion-Titanium Dioxide, CRC Press, 2012.
[22] M. Niinomi, Recent metallic materials for biomedical applications, Metallurgical and Materials Transactions a-Physical Metallurgy and Materials Science, 33 (2002) 477-486.
[23] T. Matsunaga, S. Nakasono, Y. Kitajima, K. Horiguchi, ELECTROCHEMICAL DISINFECTION OF BACTERIA IN DRINKING-WATER USING ACTIVATED CARBON-FIBERS, Biotechnology and Bioengineering, 43 (1994) 429-433.
[24] T. Matsunaga, S. Nakasono, S. Masuda, ELECTROCHEMICAL STERILIZATION OF BACTERIA ADSORBED ON GRANULAR ACTIVATED CARBON, Fems Microbiology Letters, 93 (1992) 255-260.
[25] T. Matsunaga, S. Nakasono, T. Takamuku, J.G. Burgess, N. Nakamura, K. Sode, DISINFECTION OF DRINKING-WATER BY USING A NOVEL ELECTROCHEMICAL REACTOR EMPLOYING CARBON-CLOTH ELECTRODES, Applied and Environmental Microbiology, 58 (1992) 686-689.
[26] J. Jeong, C. Kim, J. Yoon, The effect of electrode material on the generation of oxidants and microbial inactivation in the electrochemical disinfection processes, Water Research, 43 (2009) 895-901.
[27] J. Jeong, J.Y. Kim, J. Yoon, The Role of Reactive Oxygen Species in the Electrochemical Inactivation of Microorganisms, Environmental Science & Technology, 40 (2006) 6117-6122.
[28] C. Liu, X. Xie, W. Zhao, N. Liu, P.A. Maraccini, L.M. Sassoubre, A.B. Boehm, Y. Cui, Conducting Nanosponge Electroporation for Affordable and High-Efficiency Disinfection of Bacteria and Viruses in Water, Nano Letters, 13 (2013) 4288-4293.
[29] J. Gehl, Electroporation: theory and methods, perspectives for drug delivery, gene therapy and research, Acta Physiologica Scandinavica, 177 (2003) 437-447.
[30] V. Schmalz, T. Dittmar, D. Haaken, E. Worch, Electrochemical disinfection of biologically treated wastewater from small treatment systems by using boron-doped diamond (BDD) electrodes - Contribution for direct reuse of domestic wastewater, Water Research, 43 (2009) 5260-5266.
[31] P.C. Maness, S. Smolinski, D.M. Blake, Z. Huang, E.J. Wolfrum, W.A. Jacoby, Bactericidal activity of photocatalytic TiO2 reaction: Toward an understanding of its killing mechanism, Applied and Environmental Microbiology, 65 (1999) 4094-4098.
[32] A.M. Zaky, B.P. Chaplin, Mechanism of p-Substituted Phenol Oxidation at a Ti4O7 Reactive Electrochemical Membrane, Environ. Sci. Technol., 48 (2014) 5857-5867.
[33] USEPA, Method 1103.1: Escherichia coli (E. coli) in water by membrane filtration using membrane-thermotolerant Escherichia coli Agar (mTEC). EPA-821-R-06-010. Washington, DC: Office of Water, US Environmental Protection Agency, (2006).
[34] T. Charbouillot, M. Brigante, G. Mailhot, P.R. Maddigapu, C. Minero, D. Vione, Performance and selectivity of the terephthalic acid probe for (OH)-O-center dot as a function of temperature, pH and composition of atmospherically relevant aqueous media, Journal of Photochemistry and Photobiology a-Chemistry, 222 (2011) 70-76.
[35] M.H. Schnoor, C.D. Vecitis, Quantitative Examination of Aqueous Ferrocyanide Oxidation in a Carbon Nanotube Electrochemical Filter: Effects of Flow Rate, Ionic Strength, and Cathode Material, Journal of Physical Chemistry C, 117 (2013) 2855-2867.
[36] L. Guo, Y. Jing, B.P. Chaplin, Development and characterization of ultrafiltration TiO2 Magneli phase reactive electrochemical membranes, Environ Sci Technol, 50 (2016) 1428-1436.

[37] J.O. Bockris, T. Otagawa, THE ELECTROCATALYSIS OF OXYGEN EVOLUTION ON PEROVSKITES, Journal of the Electrochemical Society, 131 (1984) 290-302.
[38] R. Jurczakowski, C. Hitz, A. Lasia, Impedance of porous Au based electrodes, Journal of Electroanalytical Chemistry, 572 (2004) 355-366.
[39] D. White, The Physiology of Prokaryotes, 2nd ed., Oxford University Press, New York, 2000.
[40] Y. Hong, D.G. Brown, Electrostatic behavior of the charge-regulated bacterial cell surface, Langmuir, 24 (2008) 5003-5009.
[41] A.F. Mendonca, T.L. Amoroso, S.J. Knabel, DESTRUCTION OF GRAM-NEGATIVE FOOD-BORNE PATHOGENS BY HIGH PH INVOLVES DISRUPTION OF THE CYTOPLASMIC MEMBRANE, Applied and Environmental Microbiology, 60 (1994) 4009-4014.
[42] B.P. Chaplin, Critical Review of Electrochemical Advanced Oxidation Processes for Water Treatment Applications, Environ. Sci.: Processes Impacts, 16 (2014) 1182-1203.
[43] S.T. Sultana, E. Atci, J.T. Babauta, A.M. Falghoush, K.R. Snekvik, D.R. Call, H. Beyenal, Electrochemical scaffold generates localized, low concentration of hydrogen peroxide that inhibits bacterial pathogens and biofilms, Scientific Reports, 5 (2015).
[44] J. Iniesta, P.A. Michaud, M. Panizza, G. Cerisola, A. Aldaz, C. Comninellis, Electrochemical oxidation of phenol at boron-doped diamond electrode, Electrochim. Acta, 46 (2001) 3573-3578.
[45] D. Mishra, Z.H. Liao, J. Farrell, Understanding Reductive Dechlorination of Trichloroethene on Boron-Doped Diamond Film Electrodes, Environ. Sci. Technol., 42 (2008) 9344-9349.
[46] P.C. Foller, C.W. Tobias, THE ANODIC EVOLUTION OF OZONE, Journal of the Electrochemical Society, 129 (1982) 506-515.
[47] S. Stucki, H. Baumann, H.J. Christen, R. Kotz, PERFORMANCE OF A PRESSURIZED ELECTROCHEMICAL OZONE GENERATOR, Journal of Applied Electrochemistry, 17 (1987) 773-778.
[48] P.C. Foller, M.L. Goodwin, ELECTROCHEMICAL GENERATION OF HIGH-CONCENTRATION OZONE FOR WASTE TREATMENT, Chemical Engineering Progress, 81 (1985) 49-51.
[49] L.M. Da Silva, L.A. De Faria, J.F.C. Boodts, Eletrochemical ozone production: influence of the supporting electrolyte on kinetics and current efficiency, Electrochimica Acta, 48 (2003) 699-709.
[50] A. Kapalka, G. Foti, C. Comninellis, The importance of electrode material in environmental electrochemistry Formation and reactivity of free hydroxyl radicals on boron-doped diamond electrodes, Electrochim. Acta, 54 (2009) 2018-2023.
[51] A. Donaghue, B.P. Chaplin, Effect of Select Organic Compounds on Perchlorate Formation at Boron-doped Diamond Film Anodes, Environ. Sci. Technol., 47 (2013) 12391-12399.
[52] J.C. Crittenden, R.R. Trussell, D.W. Hand, K.J. Howe, G. Tchobanoglous, Water Treatment: Principles and Design, John Wiley and Sons, Hoboken, New Jersey, 2005.
[53] B.P. Chaplin, G. Schrader, J. Farrell, Electrochemical Destruction of N-Nitrosodimethylamine in Reverse Osmosis Concentrates using Boron-doped Diamond Film Electrodes, Environ. Sci. Technol., 44 (2010) 4264-4269.
[54] E. Veschetti, D. Cutilli, L. Bonadonna, R. Briancesco, C. Martini, G. Cecchini, P. Anastasi, M. Ottaviani, Pilot-plant comparative study of peracetic acid and sodium hypochlorite wastewater disinfection, Water Research, 37 (2003) 78-94.
[55] S. Rossi, M. Antonelli, V. Mezzanotte, C. Nurizzo, Peracetic acid disinfection: A feasible alternative to wastewater chlorination, Water Environment Research, 79 (2007) 341-350.
[56] M.T. Madigan, J.M. Martinko, K.S. Bender, D.H. Buckley, D.A. Stahl, Brock Biology of Microorganisms, 14th Edition, in, Benjamin Cummins, , 2014, pp. 165-166.
[57] H. Bergmann, T. Iourtchouk, K. Schops, K. Bouzek, New UV irradiation and direct electrolysis - promising methods for water disinfection, Chemical Engineering Journal, 85 (2002) 111-117.
[58] M.E.H. Bergmann, A.S. Koparal, Studies on electrochemical disinfectant production using anodes containing RuO2, Journal of Applied Electrochemistry, 35 (2005) 1321-1329.

[59] M.I. Kerwick, S.M. Reddy, A.H.L. Chamberlain, D.M. Holt, Electrochemical disinfection, an environmentally acceptable method of drinking water disinfection?, Electrochimica Acta, 50 (2005).
[60] A.M. Polcaro, A. Vacca, M. Mascia, S. Palmas, R. Pompei, S. Laconi, Characterization of a stirred tank electrochemical cell for water disinfection processes, Electrochimica Acta, 52 (2007) 2595-2602.
[61] C.A. Martinez-Huitle, E. Brillas, Electrochemical alternatives for drinking water disinfection, Angewandte Chemie-International Edition, 47 (2008) 1998-2005.
[62] S.N. Hussain, N. de las Heras, H.M.A. Asghar, N.W. Brown, E.P.L. Roberts, Disinfection of water by adsorption combined with electrochemical treatment, Water Research, 54 (2014) 170-178.
[63] W.Q. Guo, H. Xu, W. Yan, Ex-situ Electrochemical Disinfection with the PbO2 Anode, International Journal of Electrochemical Science, 10 (2015) 9605-9620.
[64] Electric Power Research Institute. Electricity use and management in the municipal water supply and wastewater industries, Report # 4454, (2013).

Tables and Figures

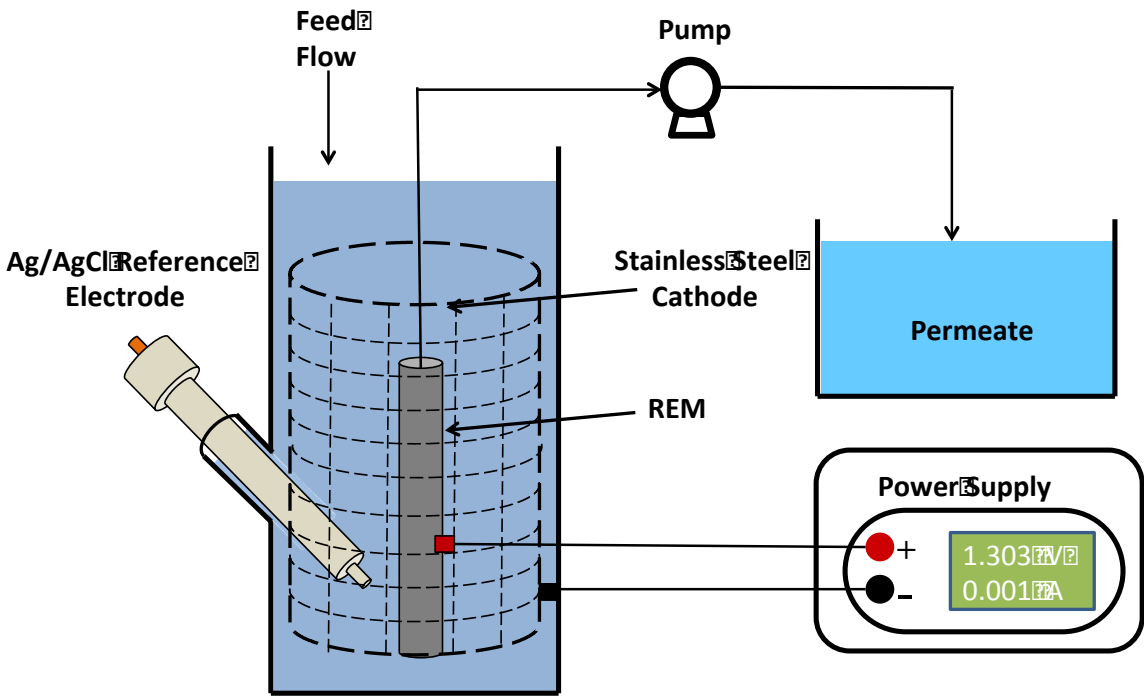

Figure 1. Schematic diagram of the membrane filtration system.

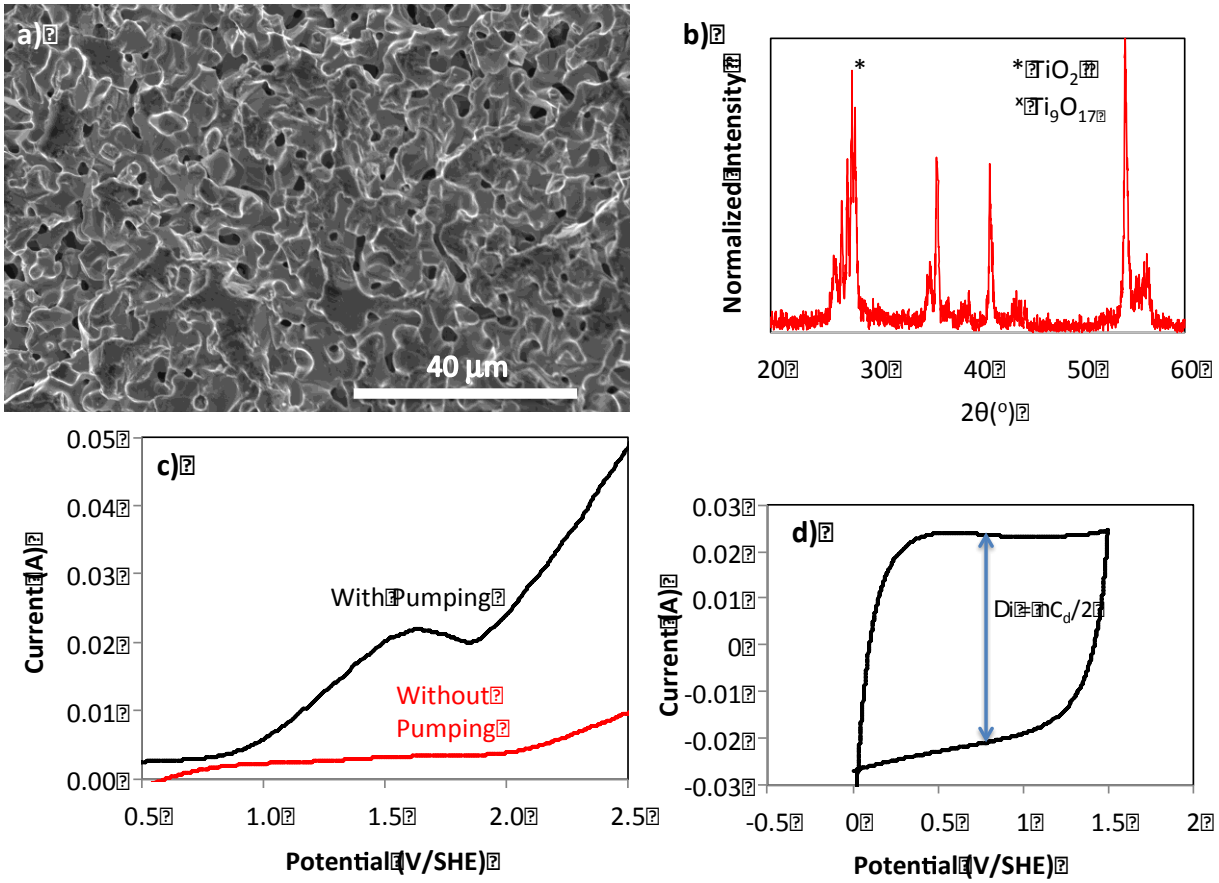

Figure 2. a) SEM image showing porous surface of the REM; b) XRD data of REM showing the characteristic TiO_2 peak; c) Linear sweep voltammetry scans (ν = 0.1 V s^{-1}) with and without pumping through the REM. Electrolyte: 100 mM KH_2PO_4, 5 mM $K_4Fe(CN)_6$ and 10 mM $K_3Fe(CN)_6$; d) CV curve showing capacitance current of the REM in 0.1 M $NaClO_4$.

* Characteristic peak for TiO_2.

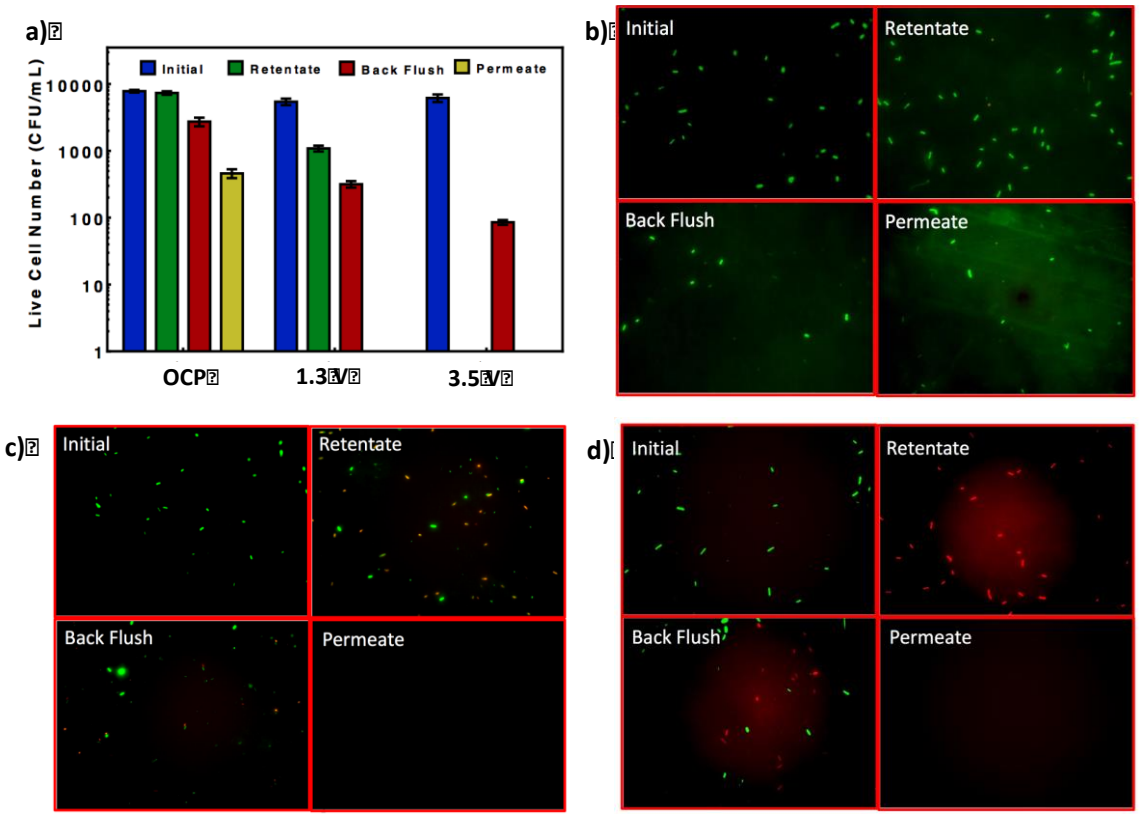

Figure 3. a) Summary of *E. coli* concentrations determined by the plate count method during filtration experiments as a function of cell potential. Fluorescent images showing live (green) and dead (red) *E. coli* cells for b) open circuit potential, c) 1.3 V cell potential, d) 3.5 V cell potential.

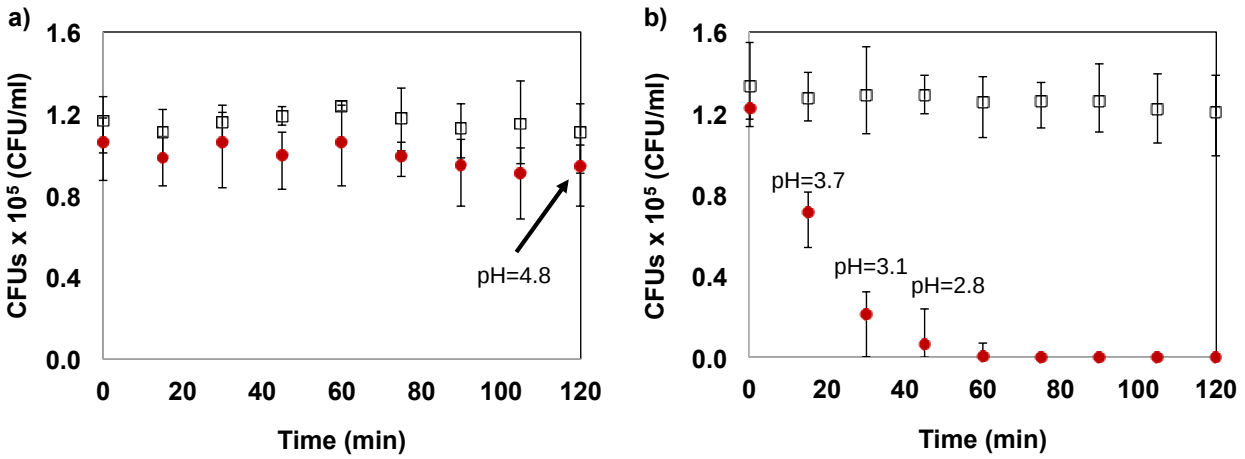

Figure 4. Bacteria concentration versus time determined by plate count method during batch inactivation experiments in a 10 mM $NaClO_4$ electrolyte: (a) 1.0 V/SHE anodic potential (b) 2.0 V/SHE anodic potential. Black squares represent control experiments conducted without an applied potential, and red dots represent experiments with an applied potential. Data points represent average values and error bars show high and low (n = 3).

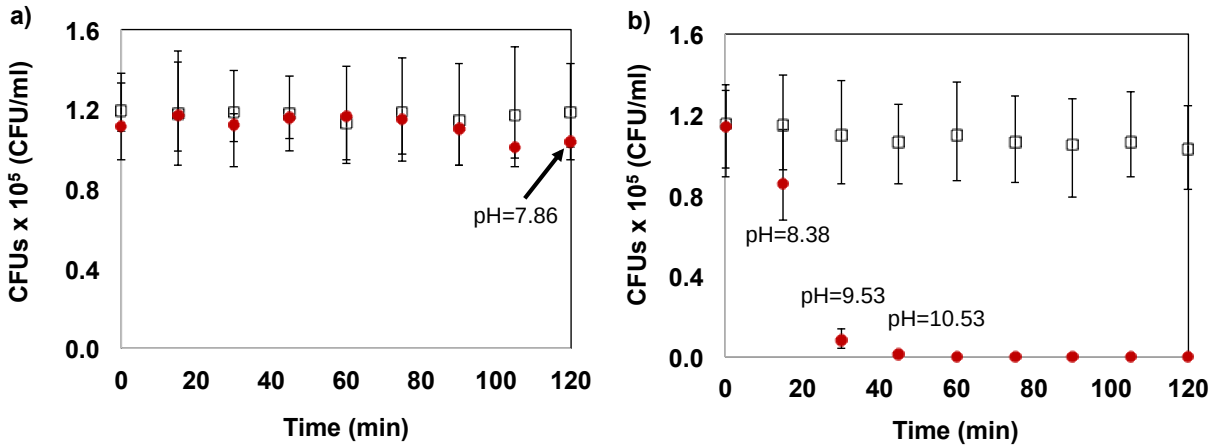

Figure 5. Bacteria concentration versus time determined by plate count method during batch inactivation experiments in a 10 mM $NaClO_4$ electrolyte: (a) -0.3 V/SHE cathodic potential (b) -1.0 V/SHE cathodic potential. Black squares represent control experiments conducted without an applied potential, and red dots represent experiments with an applied potential. Data points represent average values and error bars show high and low (n = 3).

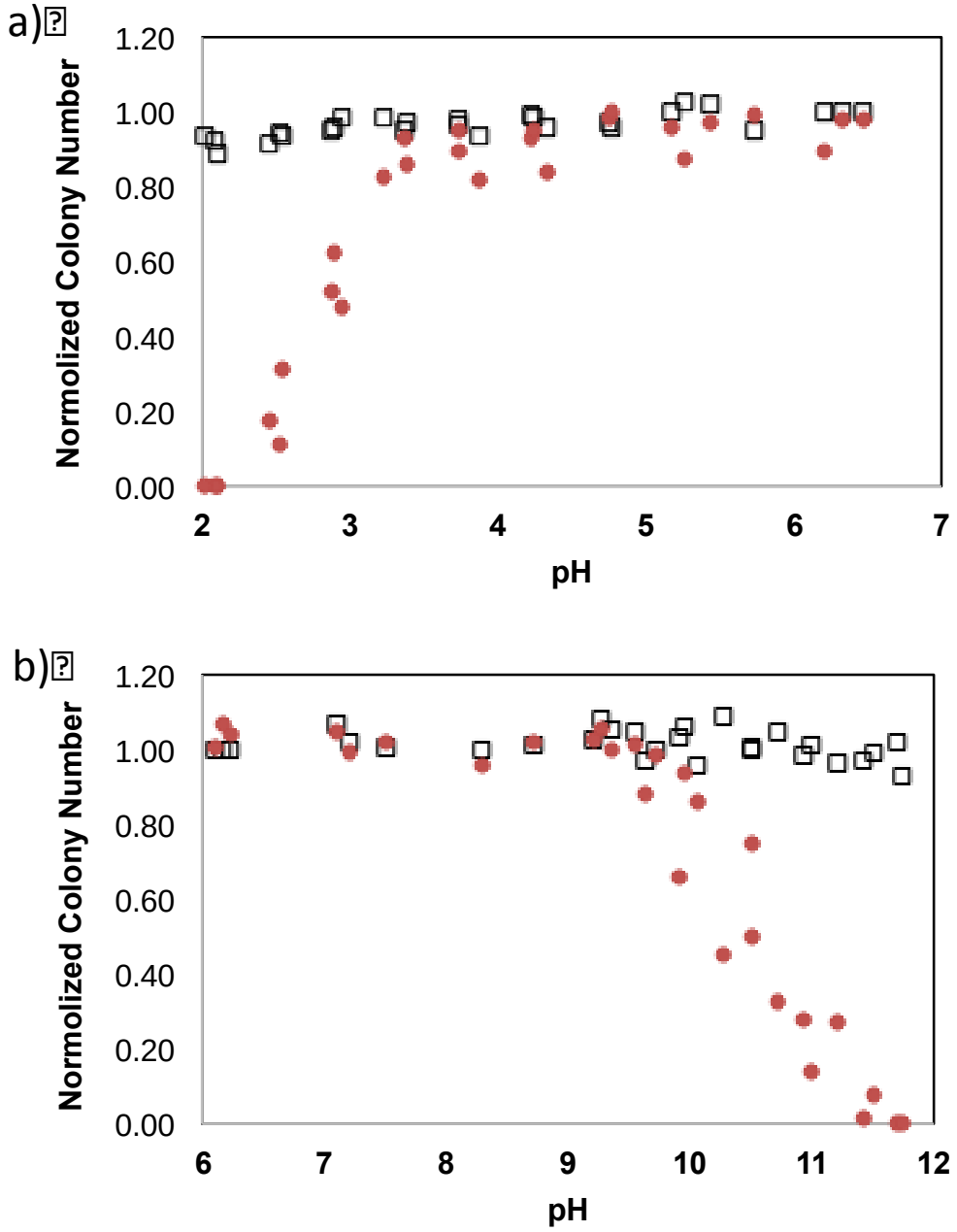

Figure 6. Bacteria concentration determined by plate count method with change of pH in a 10 mM $NaClO_4$ electrolyte: (a) Effect of acidic pH (triplicate experiments), (b) Effect of basic pH (triplicate experiments). Unfilled squares represent control experiments conducted at pH = 6.0, and red dots represent the number of bacteria in the reactor as a function of pH.

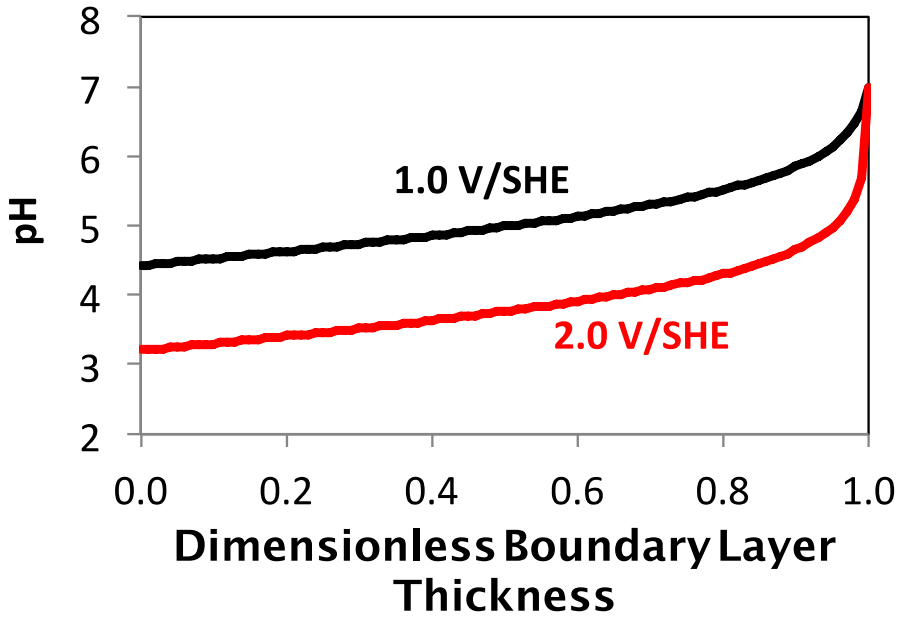

Figure 7. Profiles for pH in the boundary layer at the REM surface determined by equation (12), for anodic potentials of 1.0 V/SHE (j = 0.3 A m^{-2}) and 2.0 V/SHE (j = 5.0 A m^{-2}).